Electronic Supplementary Material (ESI) for RSC Sustainability.

Supplementary Information

Anthraquinones-Catalyzed H_2O_2 Electrosynthesis for Advanced Oxidation Process on Water Treatment

Pengdong Liu,[a, b, ‡] *Haixing Zhang,*[a, b, ‡] *Yu Chen,*[a, b, ‡] *Yajing Di,*[a, b,] *Zhilin Li,*[a, b,]

Baoning Zhu[c *], *Zheng Liu*[d *], *Zhengping Zhang,*[a, b, *] *Feng Wang*[a, b]

[a] State Key Laboratory of Chemical Resource Engineering, Beijing Key Laboratory of Electrochemical Process and Technology for Materials, Beijing University of Chemical Technology, Beijing 100029, P. R. China

[b] Beijing Advanced Innovation Center for Soft Matter Science and Engineering, Beijing University of Chemical Technology, Beijing 100029, P. R. China

[c] Beijing Engineering Center for Environmental Pollution Control and Resource Utilization, Beijing University of Chemical Technology, Beijing 100029, P. R. China

[d] State Key Laboratory of Environmental Criteria and Risk Assessment, Chinese Research Academy of Environmental Sciences, Beijing 100012, P. R. China

* Corresponding email: zhangzhengping@mail.buct.edu.cn (Z.Zhang); bnzhu@mail.buct.edu.cn (B. Zhu); liuzheng@craes.org.cn (Z. Liu)

‡ These authors contributed equally to this work.

Experimental Methods

Chemicals and materials. Isopropyl alcohol (AR) was purchased from Aladdin. C (Vulcan XC-72) was purchased from Cabot (America). PTFE emulsion (60 wt.%) was purchased from Suzhou Sinero Technology Co., Ltd. PVDF was purchased from Arkema. Triton X-100 (CP) was purchased from Sinopharm Chemical Reagent Co., Ltd. Ni foam was purchased from Kunshan guangjiayuan New Material Co., Ltd. Anhydrous sodium sulfate (AR), Sodium hydroxide (AR), Sulphuric acid (AR) and Absolute ethanol (AR) were purchased from Sinopharm Chemical Reagent Co., Ltd. Phenol (AR), 4-Hydroxy benzaldehyde (AR), p-Cresol, p-Chlorophenol (AR), p-Nitrophenol (AR) and p-hydroxybenzoic aid (AR) were purchased from Macklin. Potassium titanium(IV) oxalate (AR) was purchased from Aladdin. 9,10-anthraquinone (AR) and 1-amino anthraquinone were purchased from Adamas. Tetrabutyl titanate (AR) and Ruthenium chloride (AR) were purchased from Aladdin. Petrochemical wastewater was from Sinopec research institute of petroleum processing Co., Ltd. DSA anode was purchased from Beijing Chemical Machinery Works. Boron doped diamond anode was purchased from Anhui Zhengying Technology Co., Ltd.

Preparation of composite substrate with gas diffusion layer. For the preparation of composite substrate with gas diffusion layer, 4.86 g carbon black were mixed in the mixtures of 75 mL isopropyl alcohol and 25 mL water with ultrasonication for 30 min and stirring for 10 min. Then 5.4 mL of 60 wt.% polytetrafluoroethylene emulsion was added into the mixture, and the new mixture was high-speed stirred for 30 min to obtain

the carbon black diffusion layer slurry. The slurry was coated on the surface of the nickel foam, scraped evenly with a scraper. The modified nickel foam was completely dried at 50 °C, and then the modified nickel foam was cooled to room temperature and pressed for 1 min. The cool-pressed substrate was heated at 340 °C for 30 minutes, and the composite substrate with gas diffusion layer was obtained.

Material Characterization. The morphologies were detected by the optical microscope photograph (XS-14C, ShanghaiPuzhe) and Scanning electron microscope (FE-JSM-6701F, Japan Electronics). The X-ray diffraction (XRD) pattern of GDE were determined using a D/max-2500 X-ray diffractometer (XRD) equipped with Cu Kα radiation. Ultraviolet (UV) absorption spectroscopy was identified using a Shimadzu UV-2600i spectrometer with wavelength range from 200 to 900 nm. The chemical structure of AAQ-GDE and C-GDE were detected by X-ray photoelectron spectroscopy (XPS) (Thermo Fisher Scientific ESCALAB 250) using an Al Kα source. Fourier transform infrared spectroscopy from 4000 to 500 cm^{-1} was characterized on a Nicolet 8700/Continuum XL (Thermo Scientific). Raman spectra were carried out on a HR-800 (Horiba Jobin Yvon LabRam) using a laser of 633 nm. AFM image was carried out on S-image (SEIKO). Pore size distribution (top) and cumulative pore volume (bottom) were measured by Mercury porosimeter (AutoPore IV 9620, Micromeritics). The contact angle measurements of AAQ-GDE and C-GDE were performed using contact angle measuring instrument (OCA20, Dataphysics). Stress-strain curves was detected by AI-7000 S (Gotech testing machines (Dong Guan) Co., Ltd.).

Electrochemical experiments. Electrocatalytic H_2O_2 production was performed in a 200 mL reactor, using gas diffusion layer (4 × 4 cm^2) as cathode and boron-doped diamond (3 × 5 cm^2) as anode. Na_2SO_4 (0.1 M) was used as the supporting electrolyte. Direct electrosynthesis of H_2O_2 can be applied to environmental remediation through various processes; electro-peroxone were carried out for degrading various phenolic compounds and petrochemical wastewater. In order to achieve the goal of low energy consumption, the anode of degradation experiment adopts DSA anode (6 × 10 cm^2), the cathode and reactor are the same as those of H_2O_2 electrosynthesis. The solution pH was adjusted with H_2SO_4 and NaOH.

Analytic methods. The concentration of H_2O_2 was measured using the method of potassium titanium (IV) oxalate by UV-Vis spectrophotometer at a wavelength of 400 nm. The residual concentration of phenol was carried out by UV-Vis spectrophotometer. Specifically, take 1 ml of phenol solution, fix the volume to 25 mL, measure the characteristic absorption peak of phenol at 269.4 nm by UV-Vis spectrophotometer, and read the absorbance. COD is determined by Merck COD cell test to evaluate the index of residual organic matter in the solution. Specifically, take 3 mL of degradation solution into the COD test tube, place it in the COD digestion instrument, digest it at 165 °C for 15 min, cool it to room temperature, and measure the COD value. The energy consumption pre mass (EC) per unit COD mass (Wh g_{COD}^{-1}) using following equation.

$$EC = \frac{1000UIt}{(COD_0 - COD_t)V}$$

where U is average cell voltage (V), I is the current (A), t is reaction time (h), COD_0 is initial concentration of COD (mg L^{-1}), COD_t is the residual concentration of COD at time t (mg L^{-1}) and V is solution volume (L).

DFT Calculations. To clearly understand the reason for difference in electrochemical performances of AAQ, AQ, MAQ, and EAQ-GDE, the quantum chemical simulation was performed using the Gaussian 09 program package. The optimized geometry, electrostatic potential, and free energies (ΔG) were calculated by the density functional theory (DFT) and the B3LYP method with 6-31G(d) as the basis set. In order to obtain the ΔG of reaction step, the data obtained from the molecular structure simulation were brought into the reaction step for calculation. In order to obtain the free energies (ΔG) of each reaction step, the data obtained from the molecular structure simulation were brought into the reaction step for calculation.

Supporting Results and Discussion.

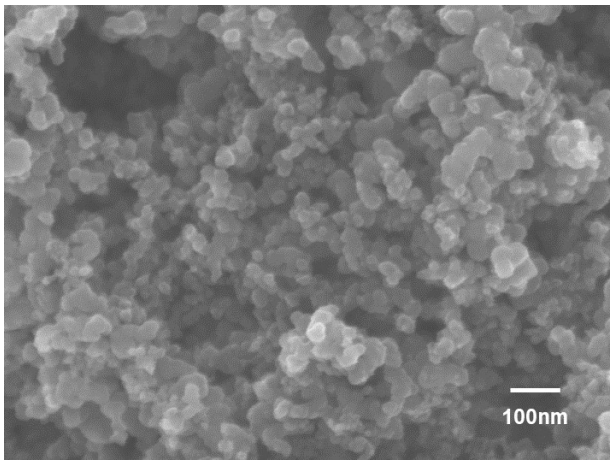

Fig. S1 SEM image of the AAQ/C.

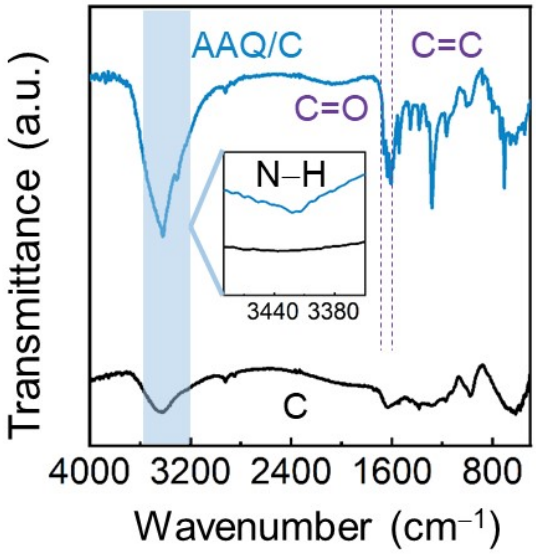

Fig. S2 FT-IR spectra of AAQ/C and C.

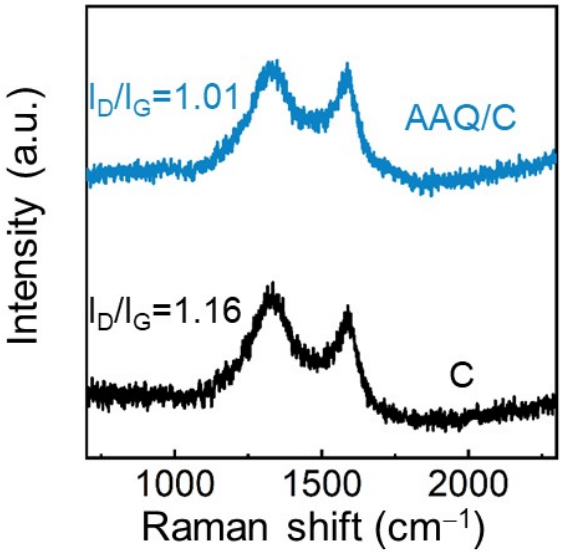

Fig. S3 Raman spectra of AAQ/C and C.

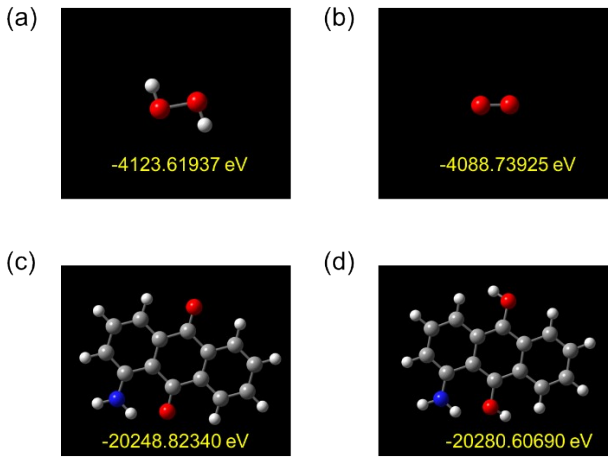

Fig. S4 DFT-optimized molecules a) H_2O_2 molecule, b) O_2 molecule, c) AAQ and d) hydro-AAQ.

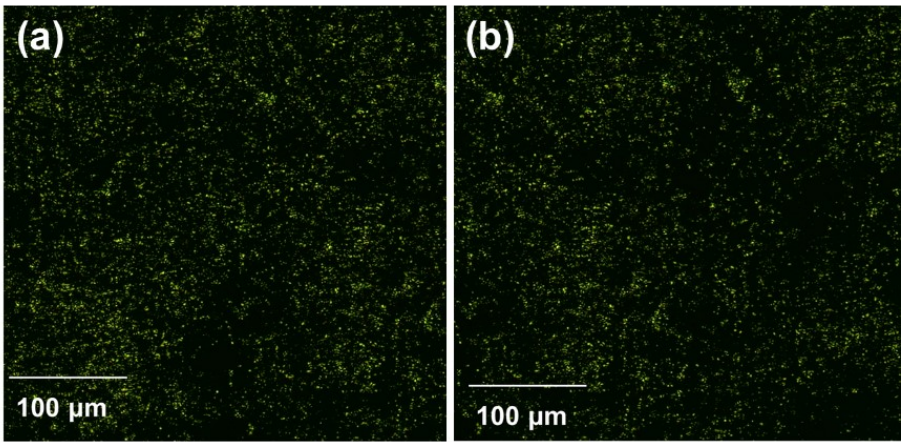

Fig. S5 Optical microscope photographs of the a) AAQ-GDE and b) C-GDE.

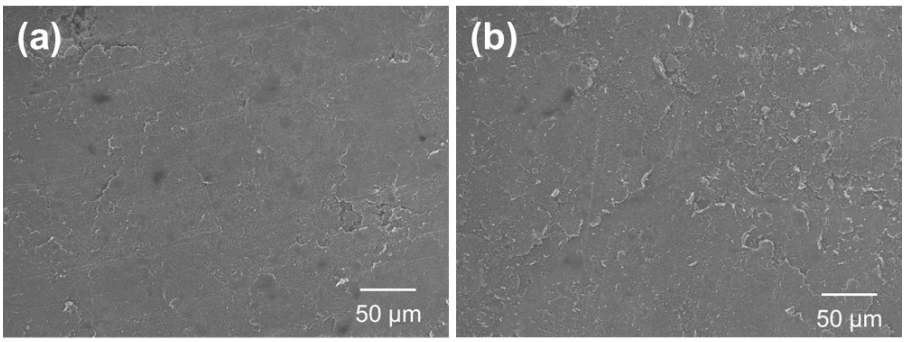

Fig. S6 SEM images of the a) AAQ-GDE and b) C-GDE surface.

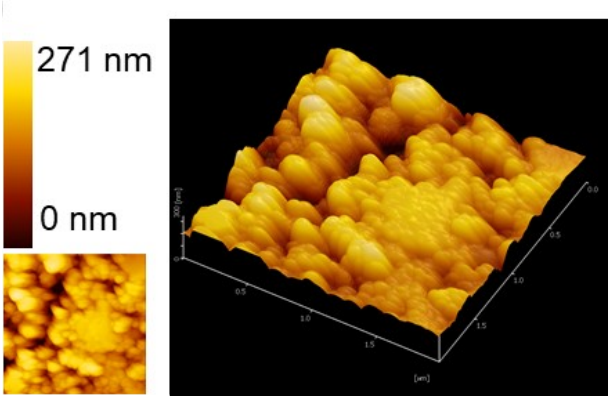

Fig. S7 AFM image of the C-GDE.

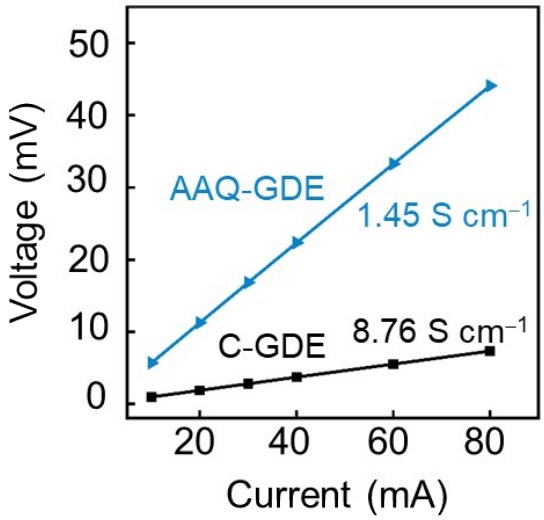

Fig. S8 The curves of current *vs.* voltage by the four–point probe measurement.

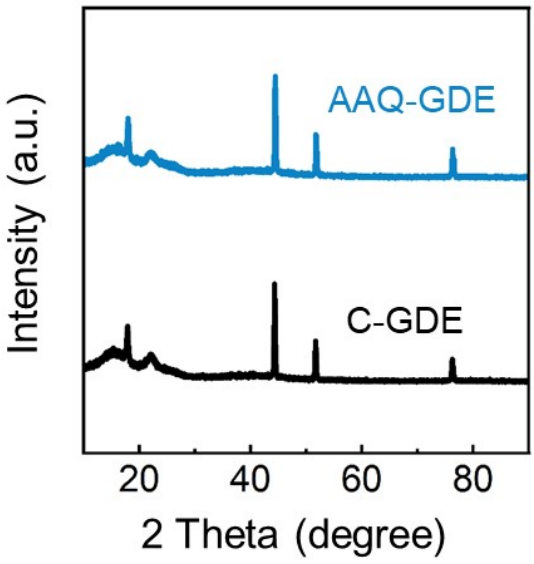

Fig. S9 XRD patterns of AAQ-GDE and C-GDE.

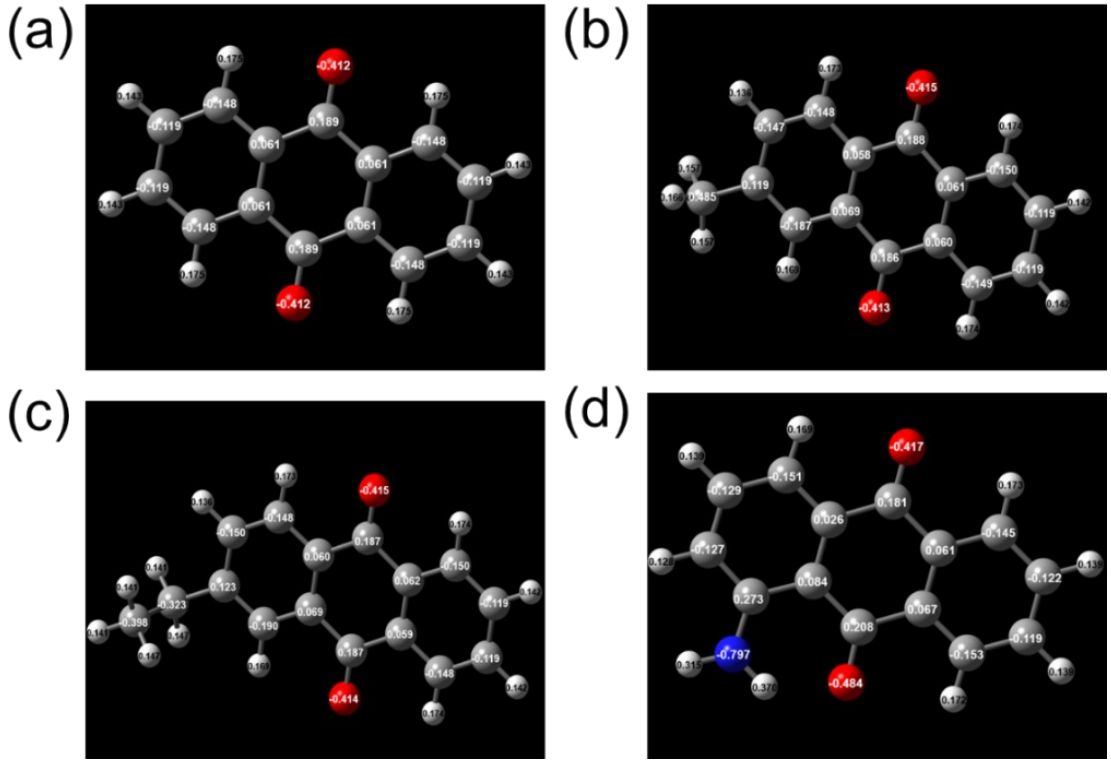

Fig. S10 Mulliken charge distribution of a) AQ, b) MAQ, c) EAQ, d) AAQ, where the gray balls represent as carbon, the red as oxygen, the blue as nitrogen, and the light gray as hydrogen.

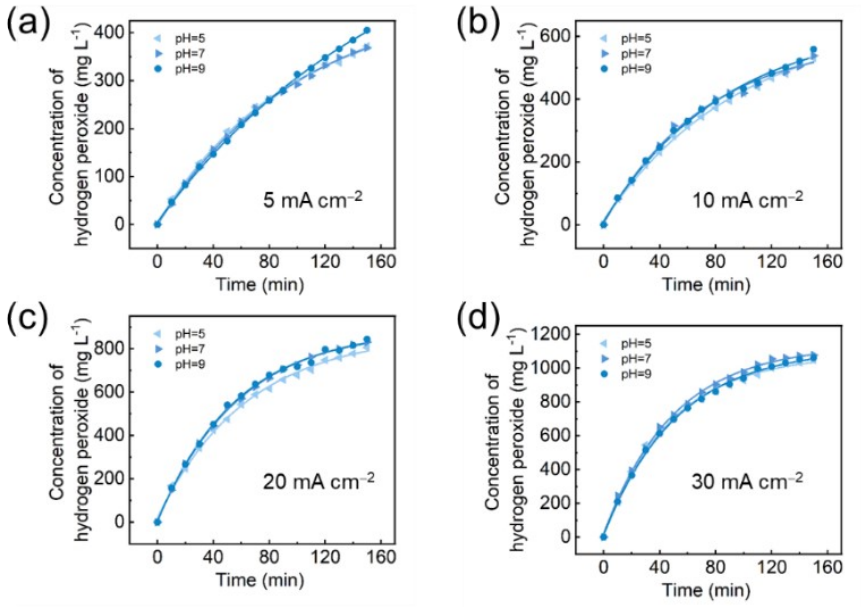

Fig. S11 H_2O_2 production in electrolyte with different pH values at different current densities for AAQ-GDE. a) 5 mA cm^{-2}, b) 10 mA cm^{-2}, c) 20 mA cm^{-2}, and d) 30 mA cm^{-2}.

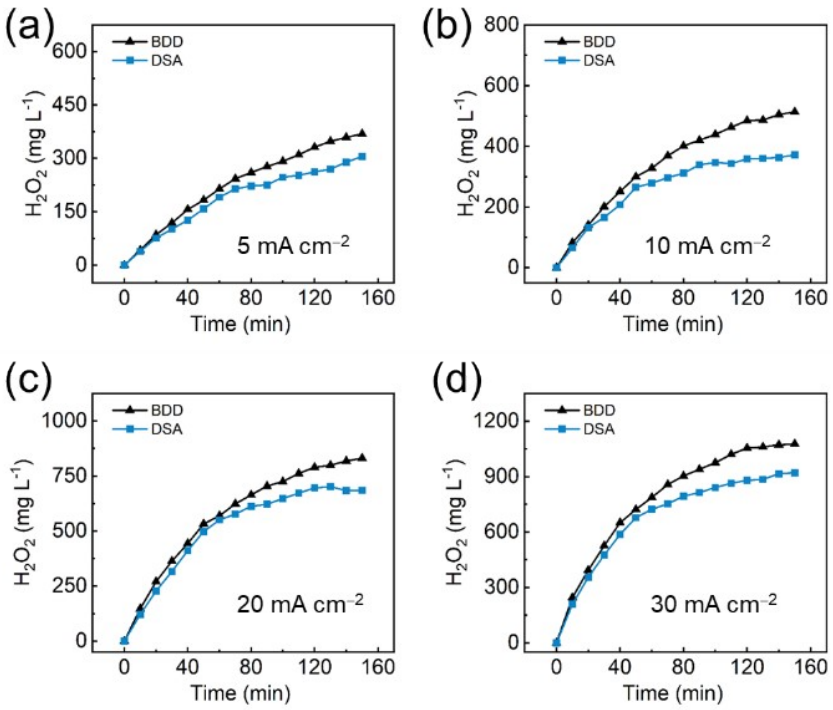

Fig. S12 H_2O_2 production at different current densities for AAQ-GDE with different anodes a) 5 mA cm^{-2}, b) 10 mA cm^{-2}, c) 20 mA cm^{-2}, and d) 30 mA cm^{-2}.

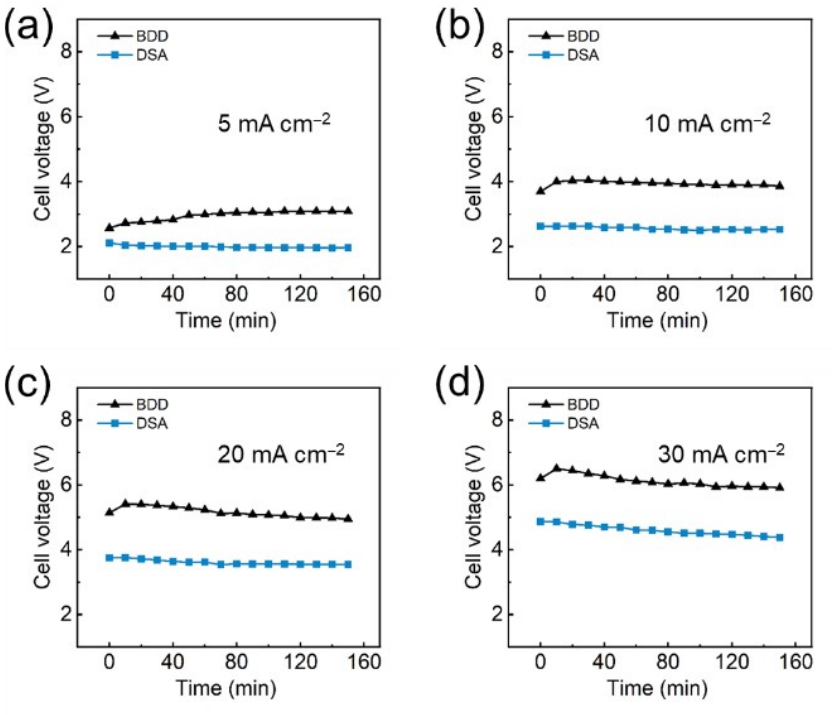

Fig. S13 Cell voltage at different current densities for AAQ-GDE with different anodes a) 5 mA cm^{-2}, b) 10 mA cm^{-2}, c) 20 mA cm^{-2}, and d) 30 mA cm^{-2}.

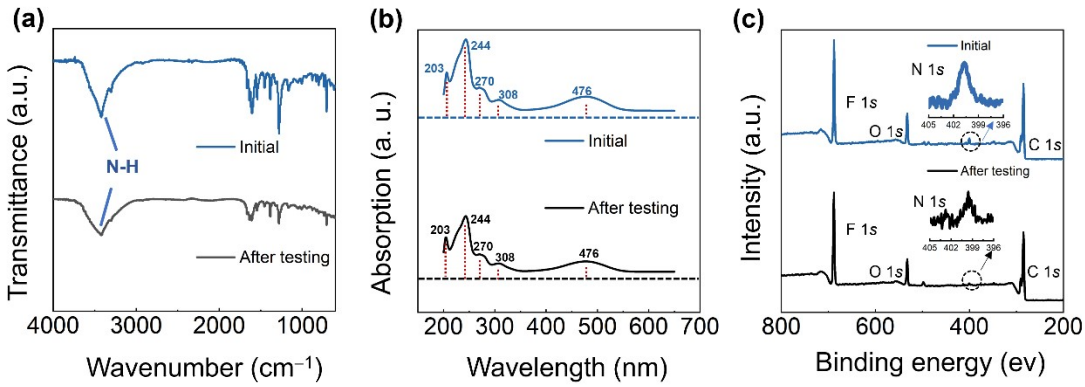

Fig. S14 a) FT-IR, b) UV-vis, and c) XPS survey spectra of AAQ-GDE before and after operation. The inset of c) is the high-resolution XPS N 1*s* spectra.

After the long-term operation, we applied FT-IR, UV-vis, and XPS spectra to measure the operated AAQ-GDE. FT-IR spectra in Fig. S14 a revealed that the peaks at 1668 cm^{-1}, 1590 cm^{-1}, and 3415 cm^{-1} were attributed to the C=O, aromatic ring, and N–H stretching, respectively, in AAQ. As shown in Fig. S14 b, the operated AAQ-GDE also exhibited the characteristic peaks similar with the initial electrode. The absorption peak at *ca.* 270 nm was attributed to quinone structure, and the other two absorption peaks at *ca.* 244 nm and 308 nm were ascribed to benzene structure. The additional absorption peak at 476 nm was attributed to the influence of the α-position amino groups. The chemical structures of AAQ-GDE before and after operation were also compared by the XPS spectra (Fig. S14 c). Both of the survey spectra and the high-resolution N 1*s* spectra confirmed that anthraquinone molecules were still preserved after the long-term operation.

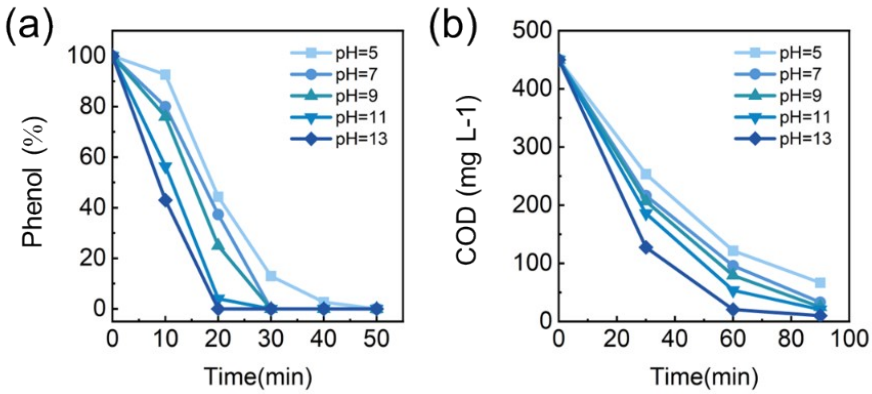

Fig. S15 a) Phenol degradation and b) COD degradation in electrolyte with different pH values (current density = 20 mA cm^{-2}).

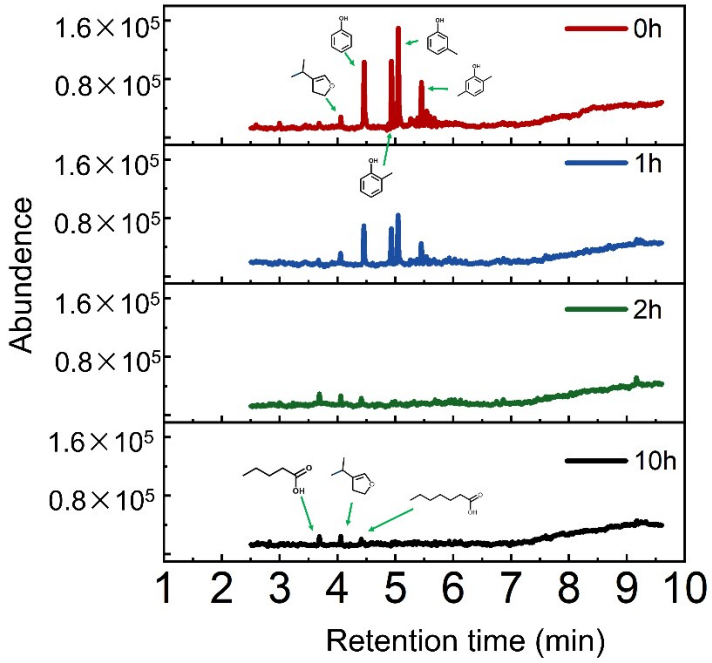

Fig. S16 Total ion chromatograms of wastewater degradation.

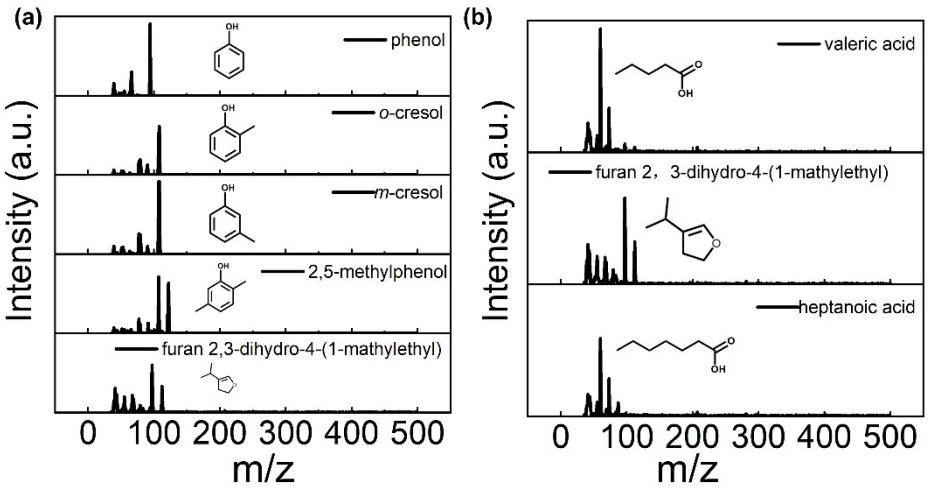

Fig. S17 Mass spectra of different samples a) at initial and b) after 10 hours.

Table S1 Calculated results of corresponding free energy of 1-amino anthraquinone oxidation and reduction reaction by using DFT method.

Reaction step	ΔE (eV)
$AAQ + 2H^+ + 2e^- \rightarrow H_2\text{-}AAQ$	0.201376
$H_2\text{-}AAQ + O_2 \rightarrow AAQ + H_2O_2$	–3.096602

Table S2 Roughness parameters of the AAQ-GDE and C-GDE.

	AAQ-GDE	**C-GDE**
r_a (nm)	46.81	36.53
r_q (nm)	153.4	120.5
r_z (nm)	253.3	185.3
P–V (nm)	398.2	343.8

Table S3 H_2O_2 productivity at different current densities.

Current density (mA cm^{-2})	**H_2O_2 productivity (mg cm^{-2} min^{-1})**
0.5	0.003
1	0.004
3	0.034
5	0.044
10	0.096
20	0.179

Table S4 Components of petrochemical wastewater.

	Basic components
Petrochemical wastewater	phenol
	o-cresol
	m-cresol
	2,5-methylphenol
	furan 2,3-dihydro-4-(1-mathylethyl)